Available online at www.sciencedirect.com
ScienceDirect
Metabolism Clinical and Experimental 59 (2010) 100 – 106
Metabolism
Clinical and Experimental
www.metabolismjournal.com

Measurement of cerebral oxidative glucose consumption in patients with type 1 diabetes mellitus and hypoglycemia unawareness using ^{13}C nuclear magnetic resonance spectroscopy

Pierre-Gilles Henry[a,*], Amy B. Criego[b,c], Anjali Kumar[b,c], Elizabeth R. Seaquist[b,c]

[a]*Department of Radiology, University of Minnesota Medical School, Minneapolis, MN 55455, USA*
[b]*Division of Endocrinology and Diabetes, Department of Medicine, University of Minnesota Medical School, Minneapolis, MN 55455, USA*
[c]*Center for Magnetic Resonance Research, University of Minnesota Medical School, Minneapolis, MN 55455, USA*

Received 14 February 2009; accepted 14 July 2009

Abstract

The aim of the present study was to use ^{13}C nuclear magnetic resonance (NMR) to measure the cerebral oxidative metabolic rate of glucose (CMRglc[ox]) in patients with diabetes and to compare these measurements with those collected from matched controls. We elected to study a group with type 1 diabetes mellitus and hypoglycemia unawareness because we had previously found such patients to have higher brain glucose concentrations than healthy volunteers under steady-state conditions. We sought to determine if this difference in steady-state brain concentrations could be explained by a difference in CMRglc(ox). Time courses of ^{13}C label incorporation in brain amino acids were measured in occipital cortex during infusion of [1-^{13}C]glucose. These time courses were fitted using a 1-compartment metabolic model to determine CMRglc(ox). Our results show that the tricarboxylic acid cycle (TCA) cycle rate (V_{TCA}, which is twice CMRglc[ox]) in subjects with type 1 diabetes mellitus was not significantly different from that of healthy controls (0.84 ± 0.03 vs 0.79 ± 0.03 μmol/[g min], n = 5 in each group, mean ± SEM). We conclude that the changes in steady-state brain glucose concentrations that we observed in patients with type 1 diabetes mellitus in a previous study (*J Neurosci Res*. 2005;79:42-47) cannot be explained by changes in oxidative glucose consumption

1. Introduction

Diabetes mellitus is a devastating disease that affects the metabolism, structure, and function of many organs. It has been long recognized that diabetes has effects on the kidneys, eyes, peripheral nerves, and vasculature; and there is a growing body of evidence that diabetes affects the brain as well [1]. Patients with diabetes have an increased incidence of cognitive dysfunction and dementia [2-4] and have been found to have abnormalities in white matter structure and function [5,6] as well as reductions in gray matter volumes and densities [7,8]. Such functional and structural abnormalities presumably result from the extremes in glycemia experienced by patients with the disease. However, the extent to which these functional and structural abnormalities are associated with or caused by alterations in glucose metabolism is uncertain. To better understand these metabolic effects, dynamic studies of the kinetics of in vivo cerebral glucose metabolism may provide new insights into how brain metabolism is altered in diabetes.

The human brain depends on the delivery of glucose from the blood to meet its metabolic needs. Glucose uptake across the blood brain barrier is dependent on the activity of glucose transporter 1; and under steady-state conditions, the rate of glucose uptake is balanced by the rate at which glucose is metabolized. Methods to assess in vivo cerebral glucose metabolism in humans have included positron emission tomography (PET) and proton nuclear magnetic resonance (NMR) spectroscopy. Both methods have contributed to our understanding of cerebral glucose metabolism, but both suffer from limitations that make it difficult to assess dynamic differences between groups of subjects with different levels of glycemia. With PET, calculation of the rates of glucose metabolism requires the use of the lump

This work was approved by the University of Minnesota Institutional Review Board: Human Subjects Committee.

* Corresponding author. Center for Magnetic Resonance Research, Minneapolis, MN 55455, USA. Tel.: +1 612 626 2001; fax: +1 612 626 2004.
E-mail address: henry@cmrr.umn.edu (P.-G. Henry).

0026-0495/$ – see front matter © 2010 Elsevier Inc. All rights reserved.
doi:10.1016/j.metabol.2009.07.012

constant, which is known to vary depending on glycemia, although changes in the lumped constant are relatively small in hyperglycemia [9]. With proton NMR, glucose transport parameters and cerebral metabolic rate of glucose (CMRglc) have been determined using steady-state measurements of brain glucose concentration at different levels of glycemia. This method, however, does not allow independent determination of the CMRglc. In contrast, ^{13}C NMR allows noninvasive determination of metabolic rates in vivo. With this method, ^{13}C glucose is administered; and the incorporation of ^{13}C label from glucose to glutamate is monitored by changes in NMR spectra. This time course of ^{13}C label incorporation from glucose to glutamate can then be used to calculate the cerebral oxidative metabolic rate of glucose (CMRglc[ox]). However, this method has not yet been applied to the study of cerebral glucose metabolism in humans with diabetes.

The aim of the present study was to use ^{13}C NMR to measure CMRglc(ox) in patients with diabetes and to compare these measurements with those collected from matched controls. We elected to study a group with type 1 diabetes mellitus and hypoglycemia unawareness because we had previously found such patients to have higher brain glucose concentrations than healthy volunteers under steady-state conditions [10]. Using ^{13}C NMR spectroscopy, we sought to determine if this difference in steady-state brain concentrations could be explained by a difference in CMRglc(ox).

2. Materials and methods

2.1. Subjects

All studies were performed following procedures approved by the Institutional Review Board at the University of Minnesota. Subjects with type 1 diabetes mellitus and hypoglycemia unawareness were recruited from the Endocrine Clinics at the University of Minnesota as described previously [10]. A clinical diagnosis was accepted, which required treatment with insulin since the year of diagnosis and a history of diabetic ketoacidosis or onset in childhood. In addition, the subjects were receiving care for diabetes labeled as type 1 by their treating physician.

Briefly, these subjects were included if they satisfied the following criteria: (1) hemoglobin A_{1c} less than 7.5%, (2) 2 self-reported episodes of hypoglycemia per week, and (3) hypoglycemia unawareness as assessed by the questionnaire developed by Clarke et al [11]. Self-reported hypoglycemia was defined as episodes when blood glucose was measured by the subject and found to be less than 70 mg/dL. The survey of Clarke et al consists of 8 questions about hypoglycemia frequency and symptoms. Subjects who indicate frequent hypoglycemia (blood glucose <70 mg/dL) without symptoms (4 or more R responses on the survey) are said to have reduced awareness of hypoglycemia. All of the subjects with type 1 diabetes mellitus in this study scored 4 or more R responses.

Control subjects were recruited from local communities around the university. The mean ± SD weight of the subjects was 68 ± 9 kg (n = 5) for the control group and 87 ± 13 kg (n = 5) for the diabetes group. The mean ± SD age was 35 ± 11 years for the control group and 44 ± 4 years for the diabetes group.

2.2. Experimental protocol

Subjects with type 1 diabetes mellitus were admitted to the General Clinical Research Center at the University of Minnesota the night before the experiment. They were taken off their long-acting insulin medication and infused with insulin during the night to maintain their blood glucose levels between 100 and 180 mg/dL. Healthy controls were asked to arrive fasted in the morning.

All subjects were studied at the Center for Magnetic Resonance Research in the morning. Venous catheters were placed in both antecubital veins for infusion of insulin, somatostatin, and glucose. A third venous catheter was placed antegrade in one foot vein for blood sampling, using warm water pads to arterialize the blood [12]. Somatostatin (0.16 mg/[kg min]) and insulin (0.5 mU/[kg min]) were infused continuously throughout the study. Unlabeled glucose was infused, and the infusion rate was adjusted to maintain glucose levels at euglycemia.

After adjustment of spectroscopic parameters, unlabeled glucose infusion was discontinued; and a 25-g bolus of [1-^{13}C]glucose (99% enriched, 50% wt/vol) was administered over 2 to 3 minutes in the right antecubital vein, immediately followed by a continuous [1-^{13}C]glucose infusion (70% enriched, 20% wt/vol). The initial rate of glucose continuous infusion was 4 mg/(kg min) and was adjusted later if necessary to keep plasma glucose around 200 mg/dL. Fig. 1 presents the time course of the protocol.

2.3. NMR spectroscopy

All experiments were performed on a 4-T/90-cm bore magnet interfaced to a Varian Inova console (Varian, Palo Alto, CA). Whole-body gradients (Siemens Sonata, Erlangen, Germany) were capable of reaching 40 mT/m in 400 microseconds. The radiofrequency coil assembly consisted of a ^{13}C surface coil (9-cm diameter) for ^{13}C detection and a quadrature ^{1}H coil for ^{1}H localization and ^{1}H decoupling. Inversion recovery turboflash T_1 images were obtained to select the volume of interest. A 5 × 3 × 3-cm^3 (45 mL) volume was chosen for spectroscopy in the visual cortex. Homogeneity of the B_0 magnetic field was optimized using FAST(EST)MAP [13] resulting in a 9- to 10-Hz water line width in the localized volume. ^{1}H-localized ^{13}C spectra were recorded using a semiadiabatic distortionless enhancement by polarization transfer (DEPT) sequence [14-16]. The ^{13}C part of DEPT consisted of a segmented BIR-4 pulse with a total duration of 4 milliseconds. The ^{1}H part of DEPT was

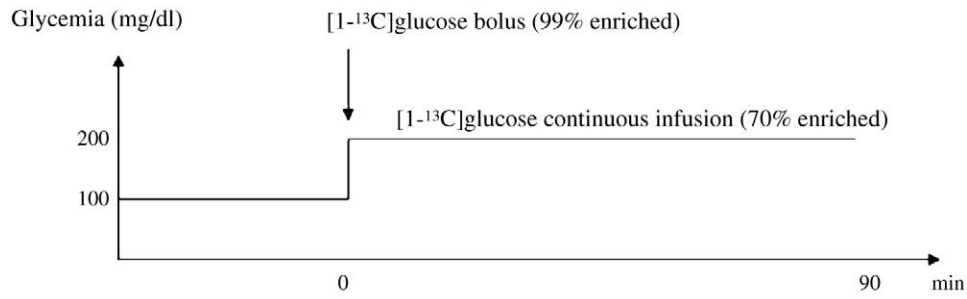

MRS adjustments	13C MRS data acquisition
^{12}C glucose	^{13}C glucose
Somatostatin (0.16 mg/kg/min)	
Insulin (0.5 mU/kg/min)	

Fig. 1. Experimental protocol. Glucose-clamp experiments were performed using somatostatin and insulin infusion. Before the infusion of ^{13}C-labeled glucose, the glucose concentration was kept at euglycemia with unlabeled ^{12}C-glucose; and NMR adjustments were performed. At $t = 0$, a bolus of 25 g of 100%-enriched 20% wt/vol [1-^{13}C]glucose solution was administered. Glucose concentration was then clamped at 200 mg/dL for the duration of the experiment using continuous infusion of 70%-enriched [1-^{13}C]glucose. Glycemia was measured every 5 minutes, and the rate of glucose infusion was adjusted to keep glycemia at the target value.

formed from 3 square pulses with a duration of 250 (90°), 500 (180°), and 125 microseconds (45°), respectively. Localization was achieved before DEPT using image-selected in vivo spectroscopy (sech/tanh pulses, 4 milliseconds' duration, 4 kHz bandwidth). Each free induction decay was collected with 3 000 complex points and a spectral width of 20 kHz resulting in an acquisition time of 150 milliseconds. ^{1}H decoupling was applied during the acquisition time using WALTZ-16 with a power of 30 W at the coil port. The available γB_1 in the voxel was approximately 3 kHz for ^{13}C (DEPT), 1 kHz for ^{1}H (image-selected in vivo spectroscopy and DEPT), and 500 Hz for ^{1}H decoupling. The frequency carrier was placed at 44 ppm for ^{13}C and 2.7 ppm for ^{1}H. Power calibrations were performed in each subject before ^{13}C infusion using the signal from ^{13}C formate in a small sphere placed at the center of the ^{13}C coil. Data were collected in blocks of 128 scans with repetition time = 3 seconds (total scan time, 6.4 minutes per block) for 80 to 90 minutes depending on subjects.

2.4. LCModel analysis

Spectra were analyzed with LCModel v6.0 (Provencher, Oakville, Ontario, Canada) [17] using a simulated basis set based on published chemical shift and J-coupling values [18]. The basis set consisted of 32 signals corresponding to multiplet signals from all isotopomers observed in the measured ^{13}C spectra (see Henry et al [18] for the nomenclature): glutamate C4S, C4D43, C3S, C3D, C3T, C2S, C2D23; glutamine C4S, C4D43, C3S, C3D, C2S, C2D23; aspartate C2S, C2D23, C3S, C3D32; alanine C3S; *N*-acetylaspartate C6S, C3S, C3D32, C2S, C2D23; GABA C4S, C2S; glucose C1α, C1β, C6α, C6β, MyoIns, GSH C4; and lactate C3. Other signals were not detectable and therefore were not included in the basis set. Time series of ^{13}C were analyzed automatically to yield time courses for each isotopomer. For metabolic modeling, the total glutamate C4 and total glutamate C3 were determined as tGluC4 = GLuC4S + GluC4D43 and tGluC3 = GluC3S + GluC3D + GluC3T. Concentrations obtained from LCModel (in arbitrary units) were converted into actual ^{13}C concentrations by assuming a glutamate concentration of 10 mmol/L and an estimated 20% isotopic enrichment (corresponding to 2.0 mmol/L ^{13}C concentration) for total glutamate C4 at isotopic steady state. In other words, this scaling was done so that the measured glutamate C4 turnover curve reaches 2.0 mmol/L at isotopic steady state (taken as the average of the last 3 points of the tGluC4 turnover curve to minimize the influence of noise). Any change in scaling will result in a change in the lactate dilution flux V_{DIL}, but has little impact on other fluxes, provided glutamate C4 and glutamate C3 curves are scaled consistently with one another. For each subject, all data points of the glutamate C4 and glutamate C3 curves were multiplied by the same scaling factor. An additional 10% scaling factor was subsequently applied to the glutamate C3 curve to account for reduced detection efficiency due to off-resonance effects, as determined on phantom.

2.5. Metabolic modeling

Time courses of incorporation of ^{13}C label into glutamate C4 and C3 were analyzed with the 1-compartment metabolic model shown in Fig. 2 using SAAM II software (University of Washington, WA). This model is similar to 1-compartment models used in previous studies [19] and accounts for the formation of ^{13}C-labeled glutamate at the C4 and C3 position from [1-^{13}C]glucose. Because glutamate is located primarily in neurons, this model reflects primarily neuronal

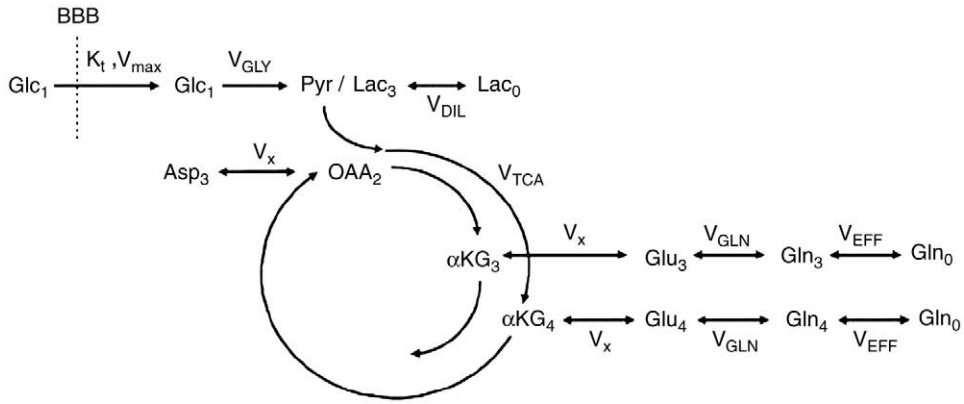

Fig. 2. Metabolic model. One-compartment metabolic model used to analyze ^{13}C turnover curves and determine the rate of TCA cycle. The model described the flow of ^{13}C label from glucose C1 to glutamate C4 and C3. Loss of label occurs by dilution through exchange with unlabeled lactate and glutamine (Lac_0 and Gln_0, respectively). Parameters V_{TCA}, V_X, V_{DIL}, and V_{EFF} were left as free parameters in the fit. Other fluxes were assumed: $V_{GLY} = 0.5 \times V_{TCA}$ and $V_{GLN} = 0.41 \times V_{TCA}$.

metabolism. Unknown (free) parameters include V_{TCA} (neuronal tricarboxylic acid cycle [TCA] cycle), V_X (exchange rate between 2-oxoglutarate and glutamate), and V_{OUT} (dilution of labeled ^{13}C lactate through exchange with unlabeled lactate). A fourth dilution flux (V_{EFF}) was added to account for loss of ^{13}C-labeled glutamine through exchange with unlabeled glutamine. This is necessary because the isotopic enrichment of glutamate C3 remains much lower than the isotopic enrichment of glutamate C4 even at isotopic steady state, indicating loss of label between the first turn and the second turn of the TCA cycle [20]. Some (but not all) of the label loss can be accounted for by pyruvate carboxylase activity. The following concentrations were assumed in the model [21]: [Glu] = 10 mmol/L, [Gln] = 2.5 mmol/L, [OAA] = 1 mmol/L, [Lac] = 1 mmol/L. Finally, the following fluxes where assumed in the model based on previous studies [21]: $V_{GLN} = 0.41 * V_{TCA}$, where V_{GLN} is the rate of glutamine synthesis, and $V_{GLY} = 0.5 * V_{TCA}$, where V_{GLY} is the rate of glycolysis, accounting for the fact that 1 molecule of glucose gives 2 molecules of lactate.

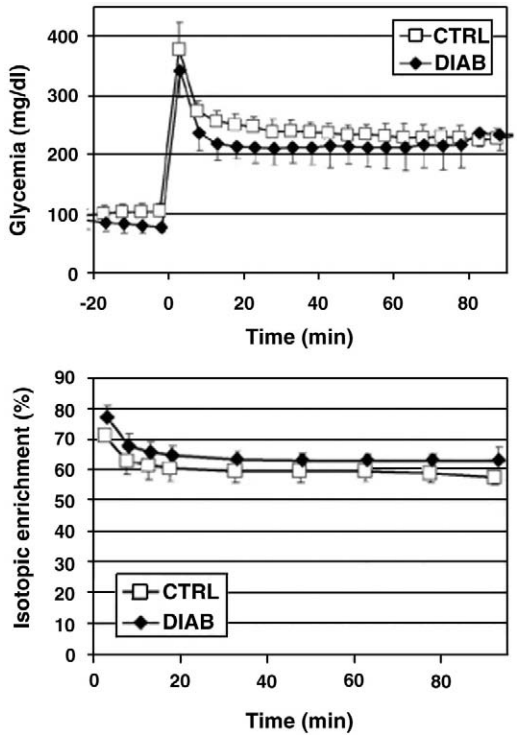

Fig. 3. Plasma glucose concentration and isotopic enrichment. Measured blood glucose concentration (top) and isotopic enrichment (bottom) in the control group (empty squares) and in type 1 diabetes mellitus group (filled diamonds). The ^{13}C glucose infusion was started at $t = 0$.

3. Results

The time courses of blood glucose concentration and isotopic enrichment were similar in the control group and the

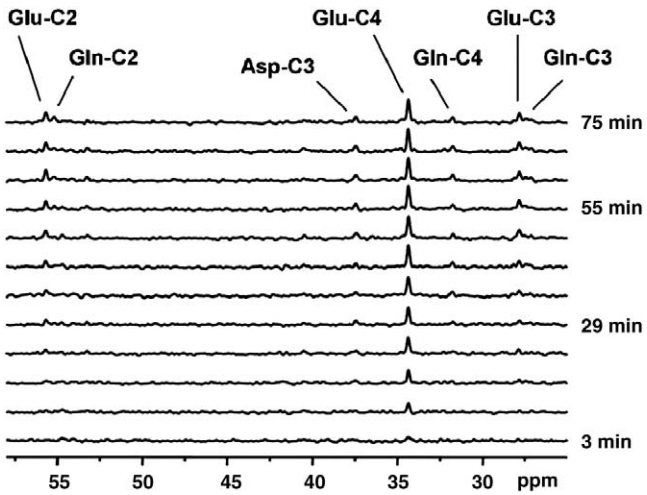

Fig. 4. Example of time course measured in one healthy volunteer. Representative time course of ^{13}C label incorporation into brain amino acids during infusion of [1-^{13}C]glucose in a single control subject (5 × 3 × 5 cm^3 volume) with a temporal resolution of approximately 6 minutes. Resonances were observed for glutamate C4, C3, C2; glutamine C4, C3, C2; and aspartate.

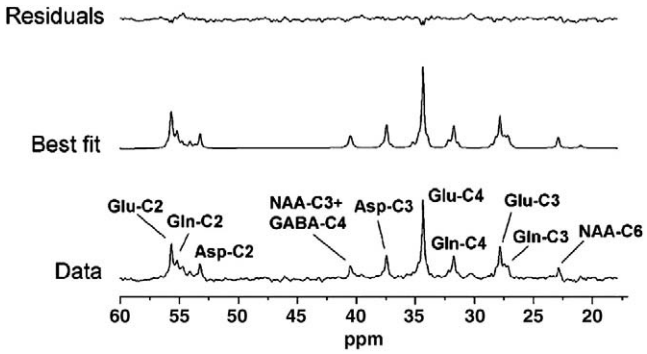

Fig. 5. LCModel analysis of ^{13}C spectrum. Example of spectral analysis of ^{13}C spectrum in human brain using LCModel with experimental data (bottom), best fit (middle), and fit residuals (top). The basis set for LCModel consisted of 32 basis spectra (see "Materials and methods" for details). The spectrum corresponds to the last 18 minutes of acquisition (3•128 scans) in a single subject and is displayed with 5-Hz line broadening.

diabetes groups (Fig. 3). Blood glucose concentration increased from approximately 100 mg/dL before the bolus of ^{13}C-labeled glucose to approximately 350 mg/dL immediately after the bolus. Blood glucose concentration was then maintained at around 200 to 250 mg/dL in both groups. Plasma glucose isotopic enrichment reached 70% to 80% immediately after the bolus then stabilized at approximately 60% to 65% for the duration of the study. Isotopic enrichment was slightly lower in the control group compared with the diabetes group. Fig. 4 shows a time series of ^{13}C spectra collected from a 4-mL volume in the occipital cortex of a control subject after injection of [1-^{13}C]glucose. Incorporation of ^{13}C label into brain amino acids is evidenced from the progressive signal increase corresponding to glutamate C4, C3, C2; glutamine C4, C3, C2; and aspartate C3 and C2 resonances. The C4 of glutamate labeled more rapidly than C3 and C2, consistent with C3 and C2 being labeled after one more turn in the TCA cycle. These time series of spectra were quantified automatically using LCModel. Fig. 5 shows LCModel analysis of a spectrum with high signal-to-noise ratio (average of all 5 control subjects and last 3 time points of time courses, corresponding to 92 minutes total scan time). Excellent localization

Table 1
Values of metabolic fluxes corresponding to best fits of ^{13}C NMR data (in micromoles per gram per minute)

	Control		Diabetes		Control vs diabetes
	Mean	SEM (n = 5)	Mean	SEM (n = 5)	*P* value (2-tailed unpaired *t* test)
V_{TCA}	0.79	0.03	0.84	0.03	.15
V_X	1.32	0.33	2.31	0.78	.44
V_{DIL}	0.21	0.06	0.29	0.06	.38
V_{EFF}	0.18	0.06	0.31	0.09	.28

performance is confirmed by the absence of natural-abundance lipid signal from the scalp.

Time courses of incorporation of ^{13}C label from [1-^{13}C] glucose into glutamate C4 and C3 appeared similar in healthy volunteers and in diabetic patients (Fig. 6). Time courses of ^{13}C label incorporation onto glutamate C4 and C3 were fitted with a 1-compartment metabolic model (Fig. 2) to determine the TCA cycle rate, V_{TCA}, as well 3 other fluxes: V_X, V_{OUT}, and V_{EFF}. The resulting metabolic fluxes are shown in Table 1. No significant difference was found between the 2 groups.

4. Discussion

We report here the first measurement of CMRglc(ox) in diabetic patients using ^{13}C NMR spectroscopy. The results show that CMRglc(ox), which is equal to 2 times V_{TCA}, is the same in patients with type 1 diabetes mellitus as it is in healthy controls. These results confirm the findings of previous studies done using PET and suggest that the limitations associated with the use of a lump constant that is known to change under different conditions of glycemia may not have much of an impact on the measurement of glucose metabolism in patients with diabetes. One advantage of ^{13}C NMR is that it does not expose humans to radioactivity.

The subjects with diabetes included in this study all had hypoglycemia unawareness, a dangerous clinical syndrome in which patients do not develop symptoms of low blood glucose until they develop neuroglycopenia. Why patients

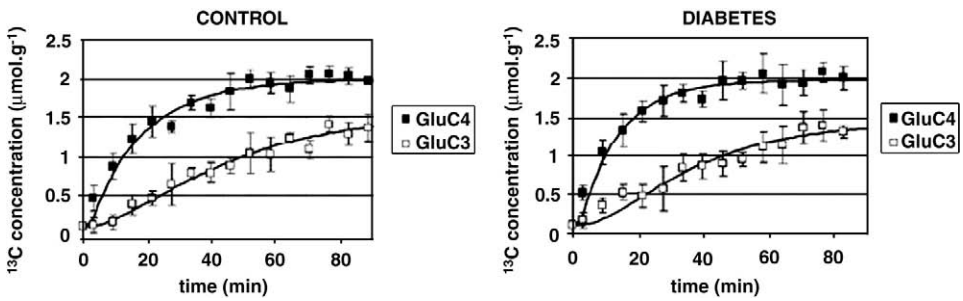

Fig. 6. Glutamate C4 and C3 time courses and fits. Experimental data for glutamate C4 (filled squares) and glutamate C3 (open squares) in control subjects (left) and in subjects with type 1 diabetes mellitus (right). Time courses of ^{13}C label incorporation were very similar in both groups. Best fits of the metabolic model to the data are shown as continuous lines. Values of metabolic rates V_{TCA} and V_X corresponding to the best fits are given in Table 1.

with diabetes and recurrent hypoglycemia develop hypoglycemia unawareness is far from clear. One mechanism that has been studied extensively is that recurrent hypoglycemia might increase glucose transport across the blood brain barrier, creating a situation in which the brain has an adequate amount of glucose for its energy needs despite a reduction in glucose content in the blood. The data reported in this article provide some support for this hypothesis of up-regulated glucose transport. If, as the current data suggest, CMRglc(ox) is the same in subjects with type 1 diabetes mellitus and hypoglycemia unawareness as it is in controls, then the 17% increase in steady-state brain glucose concentration from 4.7 to 5.5 mmol/L found by Criego et al [10] cannot be explained by changes in CMRglc(ox), suggesting that glucose transport in these subjects is up-regulated. The alternative explanation for increased steady-state brain glucose concentration would be down-regulated CMRglc. Because we show here that CMRglc(ox) is unchanged, this would imply down-regulation of nonoxidative CMRglc. However, nonoxidative glucose consumption represents only a small fraction of glucose consumption in the brain, so that a down-regulation of nonoxidative glucose consumption sufficient to explain the increase in steady-state brain glucose concentration in the Criego et al study is unlikely.

In our analysis, metabolic modeling was performed with a 1-compartment model similar to previous studies [19,22,23]. However, the current model has been adjusted to include a dilution flux for glutamine. This is justified by the fact that the enrichment of glutamate C3 remains significantly lower (about 20% lower) than the isotopic enrichment of glutamate C4, even at isotopic steady state [20]. Such a dilution of glutamate C3 compared with glutamate C4 is too large to be explained solely by pyruvate carboxylase flux. Therefore, another source of dilution must be included in the model. This is also consistent with the observation that glutamine C4 enrichment remains lower than glutamate C4 enrichment at isotopic steady state [24]. The most likely source of this dilution is the exchange of labeled glutamine with unlabeled glutamine coming from the blood. Contrary to glutamate, brain glutamine readily crosses the blood brain barrier and therefore is in exchange with the blood glutamine pool. More complex 2-compartment models have been proposed to measure compartmentalized neuronal-glial metabolism [21,25-28]. Fitting both glutamate and glutamine labeling curves has been proposed to measure the rate of glutamate-glutamine cycle between neurons and astrocytes. However, more recent work has shown that the determination of this glutamate-glutamine cycle flux is not very precise when using [1-^{13}C]glucose or [1,6-^{13}C2]glucose as a substrate [29]. Therefore, we chose to restrict our metabolic modeling to a 1-compartment model.

In our experiments, we studied subjects during modest hyperglycemia; and it is possible that a difference in V_{TCA} could have been detected between the 2 groups if subjects had been studied under hypoglycemic conditions. However, Bischof and colleagues [30] observed phosphocreatine to γ–adenosine triphosphate ratios to be the same under both euglycemia and hypoglycemia in patients with type 1 diabetes mellitus and in controls, suggesting that brain energy metabolism is not altered during hypoglycemia. Patients with type 1 diabetes mellitus have been found to have increased rates of acetate uptake during hypoglycemia when compared with controls [31], so it is possible that an up-regulation of monocarboxylic acid transport rather than an up-regulation of glucose transport could support brain energy metabolism during hypoglycemia in patients with well-controlled diabetes. Future experiments in which both glucose and acetate uptake are assessed will be necessary to determine the relative role of these substrates in the pathogenesis of hypoglycemia unawareness.

In conclusion, we used ^{13}C NMR and metabolic modeling to measure oxidative glucose metabolism in patients with type 1 diabetes mellitus and hypoglycemia unawareness and in healthy controls. We observed that V_{TCA} was the same in both groups. If these data can be used to interpret our earlier study in which steady-state brain glucose concentrations were found to be higher in unaware subjects with type 1 diabetes mellitus than controls, the current data also support the hypothesis that increased glucose transport across the blood brain barrier may be one mechanism through which subjects with type 1 diabetes mellitus and recurrent hypoglycemia develop hypoglycemia unawareness.

Acknowledgment

This work was supported by RO1NS38672 (PGH), RO1NS35192 (ERS), RO1DK62440 (ERS), P30NS057091, P41RR08679, and 5 MO1 RR0400.

References

[1] Kodl CT, Seaquist ER. Cognitive dysfunction and diabetes mellitus. Endocr Rev 2008;29:494-511.
[2] Brands AM, Biessels GJ, de Haan EH, Kappelle LJ, Kessels RP. The effects of type 1 diabetes on cognitive performance: a meta-analysis. Diabetes Care 2005;28:726-35.
[3] Leibson CL, Rocca WA, Hanson VA, Cha R, Kokmen E, O'Brien PC, et al. Risk of dementia among persons with diabetes mellitus: a population-based cohort study. Am J Epidemiol 1997;145:301-8.
[4] Ott A, Stolk RP, Hofman A, van Harskamp F, Grobbee DE, Breteler MM. Association of diabetes mellitus and dementia: the Rotterdam Study. Diabetologia 1996;39:1392-7.
[5] Kodl CT, Franc DT, Rao JP, Anderson FS, Thomas W, Mueller BA, et al. Diffusion tensor imaging identifies deficits in white matter microstructure in subjects with type 1 diabetes that correlate with reduced neurocognitive function. Diabetes 2008;57:3083-9.
[6] Manschot SM, Brands AM, van der Grond J, Kessels RP, Algra A, Kappelle LJ, et al. Brain magnetic resonance imaging correlates of impaired cognition in patients with type 2 diabetes. Diabetes 2006;55:1106-13.
[7] Musen G, Lyoo IK, Sparks CR, Weinger K, Hwang J, Ryan CM, et al. Effects of type 1 diabetes on gray matter density as measured by voxel-based morphometry. Diabetes 2006;55:326-33.

[8] Wessels AM, Simsek S, Remijnse PL, Veltman DJ, Biessels GJ, Barkhof F, et al. Voxel-based morphometry demonstrates reduced grey matter density on brain MRI in patients with diabetic retinopathy. Diabetologia 2006;49:2474-80.
[9] Schuier F, Orzi F, Suda S, Lucignani G, Kennedy C, Sokoloff L. Influence of plasma glucose concentration on lumped constant of the deoxyglucose method: effects of hyperglycemia in the rat. J Cereb Blood Flow Metab 1990;10:765-73.
[10] Criego A, Kumar A, Tran N, Tkac I, Gruetter R, Seaquist ER. Brain glucose concentrations in patients with type 1 diabetes and hypoglycemia unawareness. J Neurosci Res 2005;79:42-7.
[11] Clarke WL, Cox DJ, Gonder-Frederick LA, Julian D, Schlundt D, Polonsky W. Reduced awareness of hypoglycemia in adults with IDDM. A prospective study of hypoglycemic frequency and associated symptoms. Diabetes Care 1995;18:517-22.
[12] Seaquist ER. Comparison of arterialized venous sampling from the hand and foot in the assessment of in vivo glucose metabolism. Metabolism 1997;46:1364-6.
[13] Gruetter R, Tkac I. Field mapping without reference scan using asymmetric echo-planar techniques. Magn Reson Med 2000;43: 319-23.
[14] Gruetter R, Adriany G, Merkle H, Andersen PM. Broadband decoupled, 1H-localized 13C MRS of the human brain at 4 Tesla. Magn Reson Med 1996;36:659-64.
[15] Gruetter R, Seaquist ER, Kim S, Ugurbil K. Localized in vivo 13C-NMR of glutamate metabolism in the human brain: initial results at 4 tesla. Dev Neurosci 1998;20:380-8.
[16] Henry PG, Tkac I, Gruetter R. 1H-localized broadband 13C NMR spectroscopy of the rat brain in vivo at 9.4 T. Magn Reson Med 2003;50:684-92.
[17] Provencher SW. Estimation of metabolite concentrations from localized in vivo proton NMR spectra. Magn Reson Med 1993;30:672-9.
[18] Henry PG, Oz G, Provencher S, Gruetter R. Toward dynamic isotopomer analysis in the rat brain in vivo: automatic quantitation of 13C NMR spectra using LCModel. NMR Biomed 2003;16:400-12.
[19] Henry PG, Lebon V, Vaufrey F, Brouillet E, Hantraye P, Bloch G. Decreased TCA cycle rate in the rat brain after acute 3-NP treatment measured by in vivo 1H-[13C] NMR spectroscopy. J Neurochem 2002;82:857-66.
[20] Henry PG, Crawford S, Oz G, Ugurbil K, Gruetter R. Glucose and glial-neuronal metabolism in α-chloralose anesthetized rats measured by in vivo 13C NMR spectroscopy. Proc Intl Soc Mag Reson Med 2003;1967.
[21] Gruetter R, Seaquist ER, Ugurbil K. A mathematical model of compartmentalized neurotransmitter metabolism in the human brain. Am J Physiol Endocrinol Metab 2001;281:E100-12.
[22] Mason GF, Gruetter R, Rothman DL, Behar KL, Shulman RG, Novotny EJ. Simultaneous determination of the rates of the TCA cycle, glucose utilization, alpha-ketoglutarate/glutamate exchange, and glutamine synthesis in human brain by NMR. J Cereb Blood Flow Metab 1995;15:12-25.
[23] Mason GF, Rothman DL, Behar KL, Shulman RG. NMR determination of the TCA cycle rate and alpha-ketoglutarate/glutamate exchange rate in rat brain. J Cereb Blood Flow Metab 1992;12:434-47.
[24] Oz G, Berkich DA, Henry PG, Xu Y, LaNoue K, Hutson SM, et al. Neuroglial metabolism in the awake rat brain: CO2 fixation increases with brain activity. J Neurosci 2004;24:11273-9.
[25] Hyder F, Patel AB, Gjedde A, Rothman DL, Behar KL, Shulman RG. Neuronal-glial glucose oxidation and glutamatergic-GABAergic function. J Cereb Blood Flow Metab 2006;26:865-77.
[26] Shen J, Petersen KF, Behar KL, Brown P, Nixon TW, Mason GF, et al. Proc Natl Acad Sci U S A 1999;96:8235-40.
[27] Sibson NR, Dhankhar A, Mason GF, Behar KL, Rothman DL, Shulman RG. In vivo 13C NMR measurements of cerebral glutamine synthesis as evidence for glutamate-glutamine cycling. Proc Natl Acad Sci U S A 1997;94:2699-704.
[28] Sibson NR, Dhankhar A, Mason GF, Rothman DL, Behar KL, Shulman RG. Stoichiometric coupling of brain glucose metabolism and glutamatergic neuronal activity. Proc Natl Acad Sci U S A 1998;95:316-21.
[29] Shestov AA, Valette J, Ugurbil K, Henry PG. On the reliability of (13) C metabolic modeling with two-compartment neuronal-glial models. J Neurosci Res 2007;85:3294-303.
[30] Bischof MG, Mlynarik V, Brehm A, Bernroider E, Krssak M, Bauer E, et al. Brain energy metabolism during hypoglycaemia in healthy and type 1 diabetic subjects. Diabetologia 2004;47:648-51.
[31] Mason GF, Petersen KF, Lebon V, Rothman DL, Shulman GI. Increased brain monocarboxylic acid transport and utilization in type 1 diabetes. Diabetes 2006;55:929-34.